

Exosomes from LNCaP cells promote osteoblast activity through miR-375 transfer

SU-LIANG LI^{1*}, NA AN^{2*}, BING LIU³, SHENG-YU WANG¹, JIAN-JUN WANG⁴ and YUN YE¹

¹Department of Clinical Laboratory, The First Affiliated Hospital of Xi'an Medical University, Xi'an, Shaanxi 710077;

²Department of Laboratory Medicine, Shaanxi Jiaotong Hospital, Xi'an, Shaanxi 710068; ³Department of Pathology;

⁴Intensive Care Unit, The First Affiliated Hospital of Xi'an Medical University, Xi'an, Shaanxi 710077, P.R. China

Received April 22, 2018; Accepted December 12, 2018

DOI: 10.3892/ol.2019.10110

Abstract. Previous studies have revealed that exosomes influence tumour metastasis, diagnosis and treatment. In addition, exosomal microRNAs (miRNAs/miRs) are closely associated with the metastatic microenvironment; however, the regulatory role of exosomal miRNAs from prostate cancer cells on bone metastasis remains poorly understood. In the present study, a series of experiments were performed to determine whether exosomal miR-375 from LNCaP cells promote osteoblast activity. Exosomes were isolated and purified by ultracentrifugation, total RNA from cells and total miRNA from exosomes were then extracted, and miR-375 levels were detected by reverse transcription-quantitative polymerase chain reaction. Exosome libraries from LNCaP and RWPE-1 cells were sequenced and selected using an Illumina HiSeq™ 2500 system. The effects of exosomes on osteoblasts were determined and osteoblast activity was evaluated by measuring the activity of alkaline phosphatase, the extent of extracellular matrix mineralisation and the expression of osteoblast activity-associated marker genes. Morphological observations, particle size analysis and molecular phenotyping confirmed that cell supernatants contained exosomes. Differential expression analysis confirmed high miR-375 expression levels in LNCaP cell-derived exosomes. The ability of exosomes to enter osteoblasts and increase their levels of miR-375 was further analysed. The results demonstrated that exosomal miR-375 significantly promoted osteoblast activity. In conclusion, the present study may lead to further investigation of the function role of exosomal miR-375 in the activation and differentiation of osteoblasts in PCa.

Introduction

Prostate cancer (PCa) is a common cancer of the male urinary system, particularly in Europe and the United States (1,2). Bone is a common target for PCa metastasis, and 80-90% of advanced PCa cases present various degrees of bone metastasis (3). Approximately 50% of patients with PCa presenting bone metastases succumb within 2-3 years of diagnosis. This disease not only seriously affects the quality of life of patients, but is also associated with a heavy financial burden to society and the families of patients (4,5). Bone metastasis is a continuous, multi-step and multifactorial cascade reaction, involving the transformation of tumour cells, which react with the microenvironment. The bone metastatic process is therefore complex and remains unclear.

Exosomes are small vesicles with a diameter of 30-150 nm secreted by most cells under normal and pathological conditions (6). Early studies suggested that exosomes are used as protein transporters, which target specific receptor cells and trigger downstream signalling events (7). Studies prior to 2007 revealed that exosomes also carry nucleic acids, and are involved in intercellular communication (8). Recently, a large number of studies have confirmed that tumour-associated exosomes serve significant roles in tumour metastasis, tumour diagnosis and monitoring, and tumour therapy (9,10). Tumour cells release a large number of exosomes rich in microRNAs (miRNAs/miRs), which modify the microenvironment to facilitate tumour metastasis (11). miRNAs are non-coding, small RNA molecules that bind to the 3'-untranslated region of target mRNAs to regulate and alter the expression of target genes. Previous studies have demonstrated that mRNA expression in receptor cells is inhibited by exosome-mediated miRNAs (12,13). In addition, exosomal miRNAs secreted by cancer cells impact the status of cells at the metastatic site, which influences the formation of a metastatic microenvironment (14). Bone metastasis in PCa is closely associated with the interaction between tumour cells and the bone microenvironment, where exosomal miRNAs have an important regulatory role as signalling molecules (15). Numerous studies have reported that the expression of exosomal miRNAs is associated with PCa development (16,17). However, the regulatory role of exosomal miRNAs from PCa cells in the bone microenvironment remains poorly understood. The present

Correspondence to: Dr Yun Ye, Department of Clinical Laboratory, The First Affiliated Hospital of Xi'an Medical University, 48 West Fenghao Road, Xi'an, Shaanxi 710077, P.R. China
E-mail: yeyun236@163.com

*Contributed equally

Key words: prostate cancer, exosomes, miR-375, osteoblasts

study aimed to investigate the effects of exosomal miRNAs from PCa cells on the biological activity of osteoblasts, which are a key component of the bone microenvironment.

Materials and methods

Cell culture. LNCaP, PC-3, DU-145, 22RV1, (PCa cells lines) RWPE-1 (normal prostatic epithelial cells) and hFOB1.19 cell lines (osteoblasts) were purchased from American Type Culture Collection (Manassas, VA, USA). hFOB1.19 cells were cultured in Dulbecco's modified Eagle's medium (DMEM)/F12 (HyClone; GE Healthcare Life Sciences, Logan, UT, USA). LNCaP, PC-3, DU-145, 22RV1 and RWPE-1 cells were grown in RPMI-1640 (Gibco; Thermo Fisher Scientific, Inc., Waltham, MA, USA). All culture media were supplemented with 10% foetal bovine serum (Gibco; Thermo Fisher Scientific) and 100 U/ml penicillin and 100 mg/ml streptomycin (HyClone; GE Healthcare Life Sciences), at 37°C in 5% CO₂.

Exosome isolation. Cellular exosomes were isolated, according to a previous method (18). Cells were cultured in media supplemented with FBS depleted of exosomes. FBS depleted of exosomes were purchased from Gibco; Thermo Fisher Scientific, Inc. Supernatants were ultracentrifuged to obtain exosomes according to the protocol outlined in a previous study (7). Supernatants were collected after 48 h, centrifuged at 500 x g for 10 min and filtered (0.22 µm micropores) to remove dead cells and large debris. Subsequently, exosomes were collected, washed with PBS, ultracentrifuged at 100,000 x g for 90 min at 4°C and resuspended in PBS. NanoSight Tracking Analysis LM20 system (NanoSight Ltd., Malvern, UK) was used to examine exosome size distribution, and images of exosomes were captured with a transmission electron microscope (TEM-1400plus; JEOL Ltd., Tokyo, Japan).

Transmission electron microscopy (TEM). An aliquot of exosomes (100 µl) was diluted with PBS, and a drop of suspension was placed on a sheet of parafilm. A copper grid was placed on the drop for 2 min at room temperature and was subsequently placed onto a drop of 2% phosphotungstic acid for a 2-min staining process. The embedding resin used for TEM was HPBIO-JM3852 (purchased from Hepeng Shanghai Biotechnology Co., Ltd., Shanghai, China). The grid was air dried for several minutes and was examined using a transmission electron microscope (TEM-1400plus; JEOL Ltd.).

Flow cytometry. The exosomal pellet was diluted with filtered PBS (100 µl) and placed on ice, and the exosomal pellet samples was blocked with serum (Shanghai yuduo biotechnology Co., Ltd.) at 37°C 30 min prior to antibody incubation. The fluorescent antibodies (20 µl) against cluster of differentiation (CD)63 (1:1,000; ab134045; Abcam) and CD81 (1:1,000; ab79559; Abcam) were added for 30 min and incubated at 37°C, followed by incubation with horseradish peroxidase (HRP)-coupled goat anti-rabbit IgG H&L (1:5,000; ab6721; Abcam). The samples were stained with CD63 and CD81 separately. Unstained exosomes were used as a negative control. A BD FACSCanto II (BD Biosciences, Franklin Lakes, NJ, USA) flow cytometer was used to perform the analysis.

Differential expression analysis of exosomal miRNAs. Exosomes were collected and used to construct a cDNA library. The protocol for construction of the library: Total RNA was isolated using the TRIzol reagent (Invitrogen; Thermo Fisher Scientific, Inc.) according to the manufacturer's protocol. RNA purity was assessed using the ND-1000 Nanodrop. RNA integrity was evaluated using the Agilent 2200 TapeStation (Agilent Technologies, Inc., Santa Clara, CA, USA) and each sample had a RINe >7.0. Briefly, RNAs were ligated with 3'RNA adapter, followed by 5'adapter ligation. Subsequently, the adapter-ligated RNAs were subjected to RT-PCR and amplified with a low-cycle. The PCR products were size selected by PAGE gel according to instructions of NEBNext® Multiplex. The original 50 nt raw reads were preliminarily filtered, and clean reads were obtained through Illumina HiSeq™ 2500 sequencing (Illumina, Inc., San Diego, CA, USA). Distribution of sequence length and the consensus sequence of the sample were calculated statistically. Clean reads were classified and annotated to obtain the composition and expression information of various small RNAs in the samples. miRNA sequences were compared with known human miRNA sequences from the miRBase 21.0 database (<http://www.mirbase.org/>). Scatter plots and log₂ ratios were used to compare the co-expression of miRNAs. Edger analysis was used to analyse the significance of miRNA differences in each group (LNCaP and RWPE-1) and to calculate the P-value to screen for differentially expressed miRNAs. RStudio 1.1.463-Windows Vista/7/8/10 software was used to perform cluster analyses.

Co-culture and transduction. A lentiviral vector system encoding cytomegalovirus (CMV)-driven red fluorescent protein (RFP)-tagged CD63 (CMV-RFP-CD63) was used to label the exosomes from LNCaP or RWPE-1 cells (Shanghai SunBio Biomedical Technology Co., Ltd., Shanghai, China). Transwell chambers (0.4 mm pore filters; Sigma-Aldrich; Merck KGaA, Darmstadt, Germany) were used for the co-culture, according to the manufacturer's protocol. Osteoblasts (hFOB1.19 cells) (5x10⁴ cells) were seeded into the lower chambers, whereas LNCaP (5.0x10⁴ cells) or RWPE-1 (2.5x10⁴ cells) cells were seeded into the upper chambers and cultured for 72 h. Exosome labelling was performed using the lentiviral vector system encoding CMV-RFP-CD63 (Shanghai SunBio Biomedical Technology Co., Ltd.). A pre-experiment was conducted the day before the co-culture experiment, according to the manufacturer's protocols, and a multiplicity of infection (MOI) was determined at 100. Cells were infected with the lentivirus at MOI 100. Transwell inserts with a 0.4-mm pore-sized filter (Sigma Aldrich; Merck KGaA) for six-well plates were used according to the manufacturer's protocol.

Cell proliferation assay. Osteoblasts (hFOB1.19 cells) cultured for 24 h were serially diluted with culture medium, and absorbance values were measured following the addition of Cell Counting kit-8 (CCK-8) (Cat. No.: HY-K0301, MedChemExpress USA) reagent for 8 h 37°C, in order to produce a standard curve. Subsequently, cells were seeded in a 96-well plate (5,000 cells/100 µl/well) and 10 µl CCK-8 solution was added to each well. Cells were incubated for 4 h 37°C,

Table I. Primers against mRNAs used for RT-qPCR.

Accession Number	Gene	Primer sequence	Amplification size (bp)
NM_004967.3	BSP	F: GGCACCAGTACCAACAGCAC R: CTGCCTTCCGGTCTCTGTGG	129
NM_000582.2	OPN	F: CTGGGAGGGCTTGTTGTCA R: GTCGGCGTTTGGCTGAGAAG	105
NM_001015051.3	Runx2	F: TGAGCTCCGGAATGCCTCTG R: CTGGGTTCCCGAGGTCCATC	186
NM_002546.3	OPG	F: AGTGCAATCGCACCCACAAC R: TTCCAGCTTGCACTCACTCCA	117
NM_001256799.2	GAPDH	F: GGGTGTGAACCATGAGAAGT R: GACTGTGGTCATGAGTCCT	136

RT-PCR, reverse transcription-quantitative polymerase chain reaction.

and absorbance was measured at 450 nm using a microplate reader.

miR-375 mimics transfection. The osteoblast cells were incubated at 5×10^4 /ml in 24-well culture plates containing complete medium. Once cell density reached 30-50% confluence, cells were transfected. Briefly, 1.25 μ l 20 μ M miRNA mimics was diluted with 30 μ l 1X riboFECTTM CP Buffer and mixed (Guangzhou Ribobio Co., Ltd.). Subsequently, 3 μ l riboFECTTM CP Reagent was added to the cell culture plate and mixed slightly, and the plate was incubated at room temperature for 15 min. The riboFECTTM CP and miRNA mimics mixture was finally added to the culture plates, slightly mixed, and incubated in an atmosphere containing 5% CO₂ for 24-96 h 37°C. Finally, reverse transcription-polymerase chain reaction (RT-PCR) was used to confirm whether transfection was successful (Fig. 3B). micONTM negative control (cel-miR-239b-5p; cat. No:10000728-1-5) was used as a control (Guangzhou Ribobio Co., Ltd.); the miR-375 mimics sequence was as follows: Mimics sense: 5'-UUUGUACUACACAAA AGUACUG-3'. Mimics antisense: 5'-CAGUACUUUUGU GUAGUACAAA-3'.

Alkaline phosphatase (ALP) and Alizarin red staining. The cell suspension (200 μ l) was seeded in 24-well plates at 5×10^4 /ml and cultured for 3 weeks at 37°C in a humidified atmosphere containing 5% CO₂. Cell culture medium was changed every 2 days, medium was discarded after 2 weeks and cells were washed with PBS. Cells were then fixed for 4°C 20 min with 95% ethanol and washed three times with PBS. ALP and 0.1% Alizarin red were added (3 ml/well) (Roche Group, Swiss) at 37°C for 20 min. Cells were then washed three times with PBS, and images were assessed with a fluorescent microscope (Nikon Corporation, Tokyo, Japan; x40 magnification).

RT-quantitative PCR (RT-qPCR). Total RNA was extracted from Osteoblasts (hFOB1.19 cells) using TRIzol[®] (Invitrogen; Thermo Fisher Scientific, Inc.). Total miRNA was extracted

from exosomes using mirVana miRNA Isolation kit (Ambion; Thermo Fisher Scientific, Inc.). Total RNA was treated with TURBO DNase (Ambion; Thermo Fisher Scientific, Inc.) and cDNA was produced using the RT kit and was conducted according to the manufacturer's protocol. (Takara Biotechnology Co., Ltd., Dalian, China). Primers against mRNAs were purchased from Sangon Biotech Co., Ltd., (Shanghai, China) (Table I). Each experiment was performed in triplicate, and the mean value of the three-cycle threshold was used for further analysis. Cel-miR-39 was used as an internal control for miRNA. The expression levels of miRNA were normalised to U6, and the relative quantification was calculated using the 2^{- $\Delta\Delta$ C_q} method (19). The primers for miR-375 were as follows: Forward 5'-AGCCGTTTGTTC GTTCGGCT-3' and reverse 5'-GTGCAGGGTCCGAGGT-3'. The primers for U6 were as follows: Forward 5'-CTCGCT TCGGCAGCACACA-3' and reverse 5'-AACGCTTCACGAATT TGCGT-3'. Amplification was conducted at 95°C for 10 min, followed by 40 amplification cycles at 95°C for 10 sec and 60°C for 30 sec. The ABI Prism 7500 Sequence Detection system (Applied Biosystems; Thermo Fisher Scientific, Inc.) was used to perform qPCR (Qiagen China Co., Ltd., Shanghai, China).

Western blotting. Cells were harvested and proteins were extracted as previously described (20). A protein assay kit (Bio-Rad Laboratories, Inc., Hercules, CA, USA) was used to determine protein concentrations, and 2 mg/ml samples were loaded onto 10% SDS-PAGE gels to separate the samples according to their molecular weight. PVDF Membranes were blocked with TBST buffer (0.05% Tween-20) at room temperature for 60 min. PVDF Membranes were incubated with rabbit monoclonal anti-Golgin subfamily A member 2 (GM130; cat. no. ab52649; Abcam, Cambridge, UK) at 1:1,000, rabbit monoclonal anti-CD9 (cat. no. ab134045; Abcam) at 1:1,000, rabbit monoclonal anti-Alix (cat. no. ab186429; Abcam), at 1:1,000 and rabbit monoclonal anti-heat shock protein (Hsp)70 (cat. no. ab181606; Abcam) at 1:1,000. All primary antibody staining was performed overnight at 4°C. Horseradish

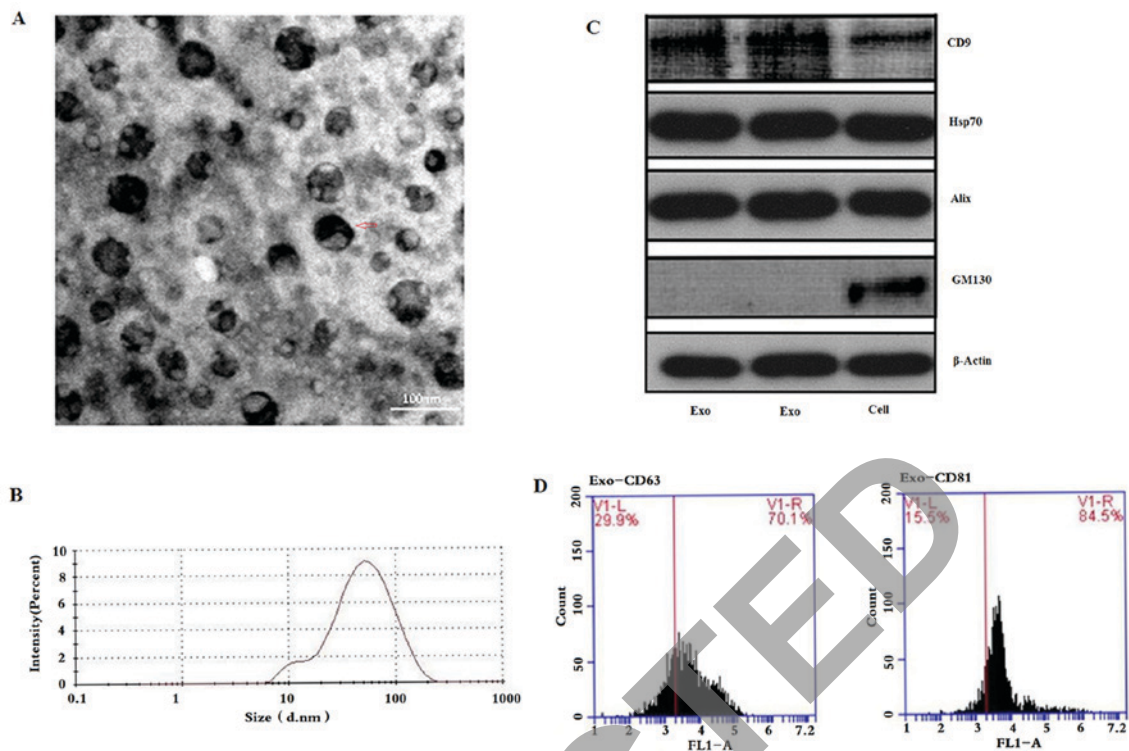


Figure 1. Purification and identification of exosomes from the LNCaP cell line. (A) Transmission electron microscopy was performed to investigate exosome size and structure. Vesicles 30–150 nm in diameter were indicative of exosomes. (B) Particle size of exosomes ranged between 30 and 150 nm, with a peak of 72 nm, as assessed by NanoSight nanoparticle analysis. (C) Expression levels of CD9, Hsp70, Alix and GM130 were detected in exosomes by western blotting (lanes 1–2, exosomal pellets; lane 3, cells). (D) Expression levels of CD63 and CD81 were detected in exosomes by flow cytometry. Scale bar, 100 nm. CD, cluster of differentiation; GM130, Golgin subfamily A member 2; Hsp70, heat shock protein 70.

peroxidase-coupled goat anti-rabbit immunoglobulin G H&L (cat. no. ab6721; Abcam) at 1:5,000 was used as a secondary antibody for 45 min at 37°C. β -actin (cat. no. mAbcam8226; Abcam) at 1:1,000 was used as a loading control. ECL was used to visualize blots (cat. no. WLA003; Wanleibio).

Statistical analysis. SPSS 18.0 software (SPSS Inc., Chicago, IL, USA) for windows was used to perform all statistical analyses. All experiments were repeated three times. The results are presented as the mean \pm standard deviation. Two-tailed Mann-Whitney U-test was used to analyse non-parametric data. Multigroup comparisons of parametric data were conducted using one-way analysis of variance (ANOVA) with Tukey's post hoc test. $P < 0.05$ was considered to indicate a statistically significant difference.

Results

Exosome identification in cell supernatants of the LNCaP cell line. As presented in the TEM images (Fig. 1A), LNCaP-isolated exosomes were round, oval or cup-shaped, lipid bilayer membranous vesicular structures (red arrow). Cell debris and cellular organelles were not observed in the entire field of view (Fig. 1A). The exosome population contained particles with a diameter between 30 and 150 nm, with a distribution peak of 72 nm (Fig. 1B). Western blotting demonstrated that exosome populations expressed common exosome protein markers, including CD9, Hsp70 and Alix; however, GM130 was not detected (Fig. 1C). Flow cytometric analysis revealed

clear expression of CD63 and CD81, with a positive expression rate of >70% (Fig. 1D).

Differential expression analysis of exosomal miRNAs. The exosome sequencing libraries of LNCaP and RWPE-1 cell lines were sequenced and filtered by Illumina HiSeq™ 2500. The sequences obtained were compared with those in the miRBase 21.0 database, in order to provide information about each miRNA and its expression levels. The percentage of miRNA in the sample was ~6.51% (Fig. 2A). Variations in miRNA expression between the groups were compared by scatter plot analysis using the log₂ ratio (Fig. 2B). Results revealed that exosomes isolated from PCa cells exhibited 298 differentially expressed genes ($\log_2(\text{fold-change}) > 1$), with 100 downregulated and 198 upregulated miRNAs, compared with exosomes from the control group (RWPE-1). Among these, 50 miRNAs demonstrated significantly different expression ($P < 0.01$), including 37 that were downregulated and 13 that were upregulated (Table II).

In addition, 50 differentially expressed miRNAs were identified, and cluster analysis could fully distinguish between the two types of exosomes (Fig. 2C). In exosomes from LNCaP cells, miR-375, miR-200c-3p and miR-141-3p expression levels were upregulated, whereas miR-100-5p, miR-584-5p and miR-125b-1-3p were downregulated (Fig. 2D). Subsequently, miR-375 levels in exosomes from PCa cells were significantly higher than those from RWPE-1.0 exosomes ($P < 0.05$; Fig. 2E).

Osteoblast activity is promoted by exosomal miR-375. CMV-RFP-CD63 lentivirus was used to infect LNCaP and

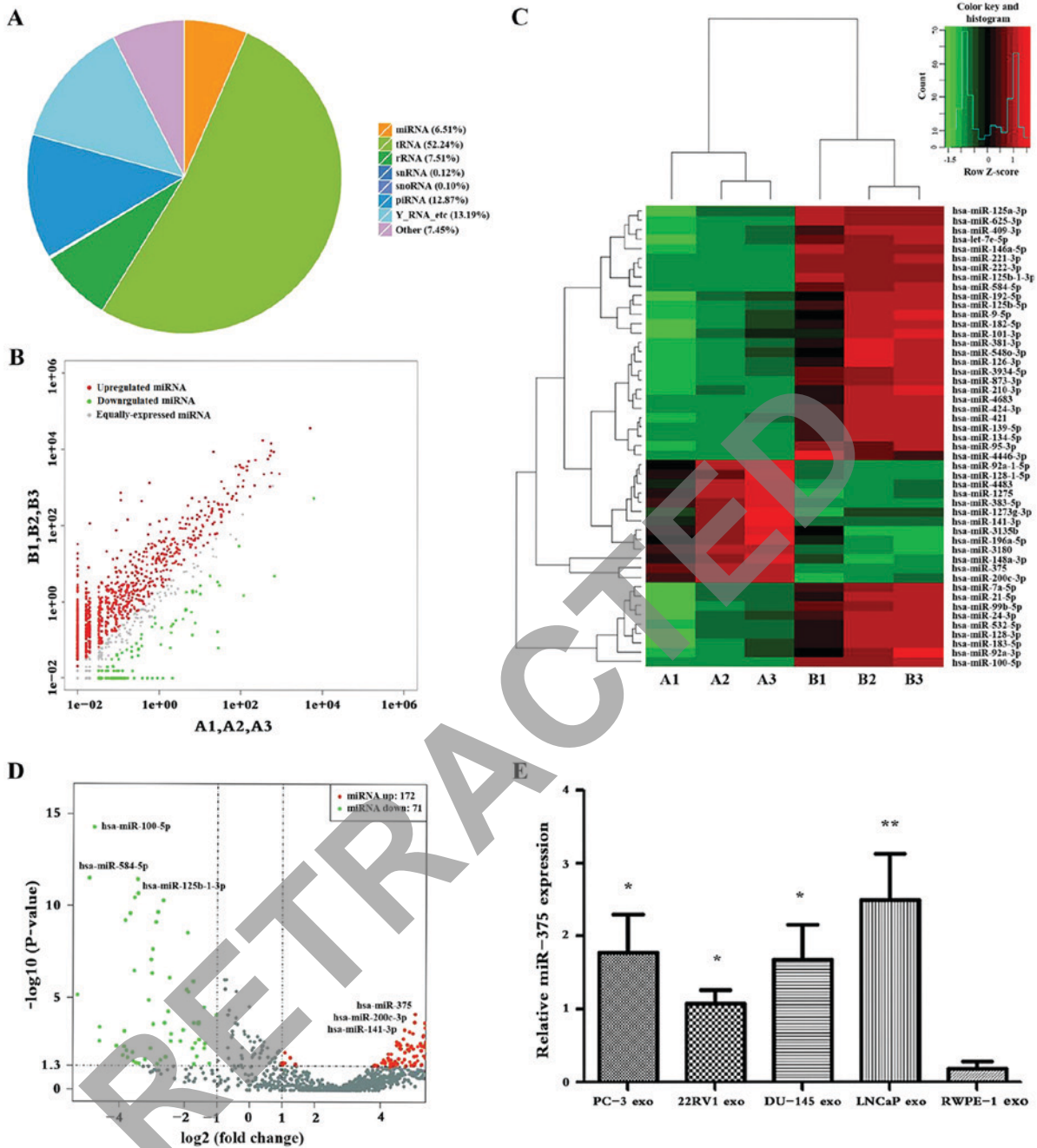


Figure 2. Differential expression of exosomal miR-375. (A) Non-coding RNA classification. The average miRNA percentage in the sample was 6.51%. (B) Scatter plot of differences in miRNA expression. The upregulated miRNAs are indicated with red dots, downregulated miRNAs are indicated with green dots, and the miRNAs that were not significantly different are indicated with grey dots. (C) Heatmap of differences in miRNA expression levels. Red, upregulated; black, intermediate value; green, downregulated. Cut-off: $|\log_2(\text{fold-change})| \geq 1$. A1, A2, A3: LNCaP cells; B1, B2, B3: RWPE-1 cells. (D) Volcano plot of differences in miRNA expression levels. Red, upregulated; grey, intermediate value; green, downregulated. (E) Relative expression levels of miR-375 in exosomes. * $P < 0.05$ and ** $P < 0.01$ vs. RWPE-1 exo. exo, exosome; miR/miRNA, microRNA.

RWPE-1 cells that would generate RFP-labelled exosomes, prior to the setting up of a co-culture system. After 72 h, a substantial level of RFP-labelled exosomes was observed in osteoblasts cultured with LNCaP cells (Fig. 3A). In addition, the expression levels of miR-375 were markedly increased in osteoblasts cultured with LNCaP cells; however, it was unclear as to whether the elevated miR-375 levels observed in osteoblasts were derived from exosomes produced by these cells. Osteoblasts were therefore treated with LNCaP-derived exosomes, as a control group. The results demonstrated that

osteoblasts treated with LNCaP-derived exosomes also exhibited high levels of miR-375 (Fig. 3B). These findings suggested that exosomes from LNCaP cells enriched in miR-375 may enter osteoblasts to increase their miR-375 expression. In addition, the proliferative activity of osteoblasts was significantly increased following co-culture with LNCaP cells (Fig. 3C).

Afterwards, osteoblasts were transfected with miR-375 mimics to determine whether the alterations in the proliferative activity of osteoblasts were associated the expression levels of exosomal miR-375 (Fig. 4). Subsequent staining revealed

Table II. Significant differences in miRNA expression between exosome samples.

miRNA_ID	LNCaP	RWPE-1	Up/Down	log2 (fold-change)	P-value
hsa-miR-375	660.546	4.847	Up	-7.090	8.65x10 ⁻²⁸
hsa-miR-200c-3p	117.042	1.454	Up	-6.330	3.34x10 ⁻²⁴
hsa-miR-100-5p	28.453	93514.788	Down	11.682	4.04x10 ⁻²⁴
hsa-miR-221-3p	0.370	438.183	Down	10.207	3.80x10 ⁻¹⁷
hsa-miR-584-5p	0.574	1336.401	Down	11.184	4.67x10 ⁻¹⁷
hsa-miR-141-3p	92.104	0	Up	-7.716	1.55x10 ⁻¹⁰
hsa-miR-383-5p	6.437	0.133	Up	-5.589	9.07x10 ⁻¹⁷
hsa-miR-125b-1-3p	0.113	737.556	Down	12.663	1.81x10 ⁻¹⁶
hsa-miR-222-3p	0.114	461.820	Down	11.971	3.09x10 ⁻¹⁶
hsa-miR-1275	7.608	0.280	Up	-4.763	5.13x10 ⁻¹⁵
hsa-miR-3180	29.633	2.739	Up	-3.435	3.44x10 ⁻¹²
hsa-miR-4483	3.830	0.357	Up	-3.420	2.01x10 ⁻¹¹
hsa-miR-148a-3p	622.901	530.226	Up	-3.529	3.59x10 ⁻¹¹
hsa-miR-4683	0.087	74.090	Down	9.727	4.86x10 ⁻¹¹
hsa-miR-92a-1-5p	4.492	0.637	Up	-2.817	2.24x10 ⁻¹⁰
hsa-miR-128-1-5p	4.455	0.609	Up	-2.869	7.79x10 ⁻¹⁰
hsa-miR-1273g-3p	6.629	1.770	Up	-1.904	2.89x10 ⁻⁰⁹
hsa-miR-146a-5p	0.989	132.748	Down	7.067	2.53x10 ⁻⁰⁸
hsa-miR-424-3p	0.591	107.159	Down	7.502	2.61x10 ⁻⁰⁷
hsa-miR-125b-5p	6.303	531.265	Down	6.397	3.38x10 ⁻⁰⁷
hsa-miR-196a-5p	26.85	3.374	Up	-2.992	4.57x10 ⁻⁰⁷
hsa-miR-134-5p	0.117	22.589	Down	7.591	3.71x10 ⁻⁰⁶
hsa-miR-3135b	17.690	4.837	Up	-1.870	4.96x10 ⁻⁰⁶
hsa-miR-873-3p	0.655	33.700	Down	5.685	9.15x10 ⁻⁰⁶
hsa-miR-95-3p	0.195	11.800	Down	5.915	3.00x10 ⁻⁰⁵
hsa-miR-210-3p	0.532	58.437	Down	6.770	4.11x10 ⁻⁰⁵
hsa-miR-99b-5p	100.091	3353.701	Down	5.066	7.11x10 ⁻⁰⁵
hsa-miR-4446-3p	0.073	13.212	Down	7.493	8.71x10 ⁻⁰⁵
hsa-miR-9-5p	4.995	336.572	Down	6.074	0.000134
hsa-miR-3934-5p	1.121	37.106	Down	5.048	0.0002
hsa-miR-421	0.493	20.191	Down	5.354	0.000215
hsa-miR-139-5p	0.425	20.522	Down	5.590	0.000249
hsa-miR-183-5p	74.134	3554.843	Down	5.583	0.000306
hsa-miR-381-3p	0.988	40.863	Down	5.370	0.000405
hsa-miR-24-3p	109.163	3243.622	Down	4.893	0.000659
hsa-miR-92a-3p	337.962	17202.180	Down	5.669	0.000722
hsa-miR-21-5p	153.241	4900.051	Down	4.998	0.000854
hsa-miR-192-5p	13.447	537.908	Down	5.322	0.001015
hsa-miR-126-3p	1.723	68.249	Down	5.307	0.001230
hsa-let-7e-5p	3.712	83.898	Down	4.498	0.002247
hsa-let-7a-5p	225.265	5351.823	Down	4.570	0.002885
hsa-miR-532-5p	114.652	3253.283	Down	4.826	0.003257
hsa-miR-625-3p	6.360	155.272	Down	4.609	0.003632
hsa-miR-125a-3p	8.542	193.385	Down	4.500	0.003711
hsa-miR-409-3p	4.524	109.785	Down	4.601	0.005114
hsa-miR-128-3p	88.752	2177.163	Down	4.616	0.005544
hsa-miR-182-5p	38.802	960.206	Down	4.629	0.005589
hsa-miR-101-3p	32.976	1446.715	Down	5.455	0.005672
hsa-miR-548o-3p	1.337	38.338	Down	4.841	0.006137

miR/miRNA, microRNA.

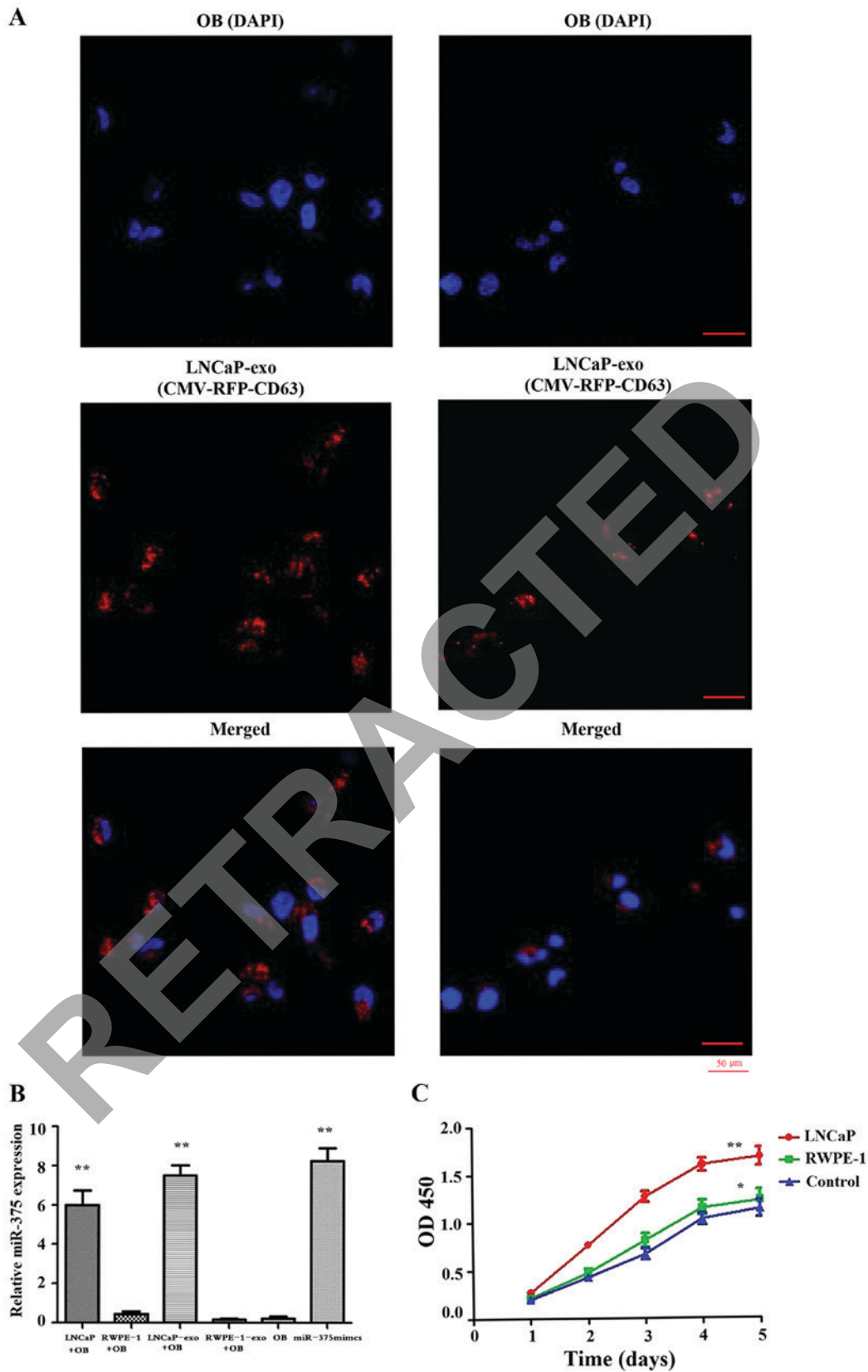


Figure 3. Effects of LNCaP-derived exosomes on osteoblasts. (A) Representative confocal images of CD63-RFP-exosomes from donor cells at 72 h after co-culture. Scale bar 50 μ m. (B) Reverse transcription-quantitative polymerase chain reaction analysis of exosomal miR-375 expression. ** P <0.01 vs. OB. (C) Effects of LNCaP-derived exosomes on osteoblast proliferation. CD63, cluster of differentiation 63; * P <0.05 and ** P <0.01 vs. Control; CMV, cytomegalovirus; exo, exosome; miR-375, microRNA-375; OB, osteoblast; OD, optical density; RFP, red fluorescent protein.

the presence of a large number of brown ALP particles in the cytoplasm (Fig. 4A). Furthermore, a significant increase in

ALP activity was observed compared with the control group that had been transfected with the negative control miRNA

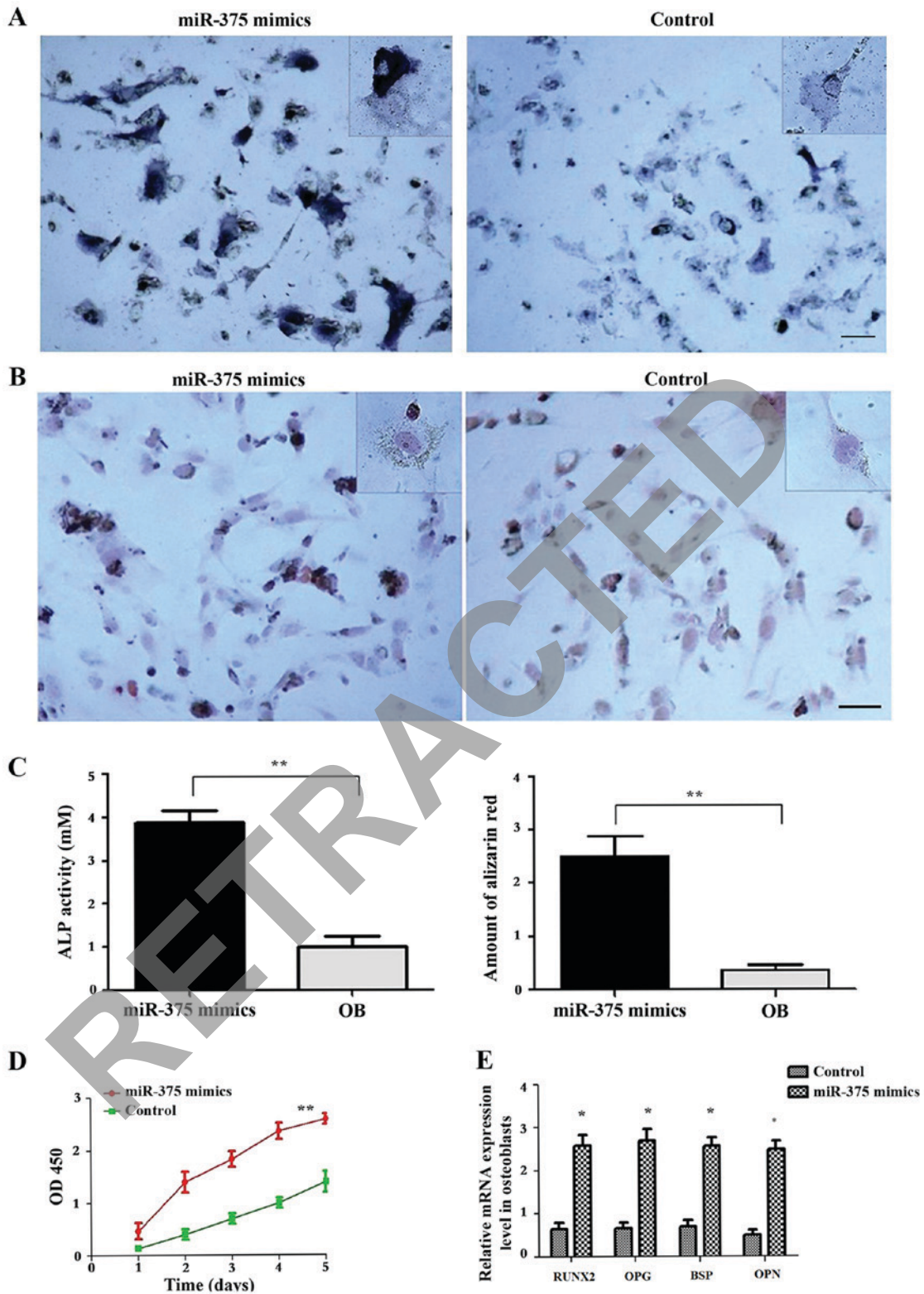


Figure 4. Effects of miR-375 mimics on osteoblast activity. (A) ALP staining. A large number of brown ALP particles was detected in the cytoplasm following transfection of osteoblasts with miR-375 mimics. Images were acquired under a microscope at x400 magnification. (B) Alizarin red staining. Deposition of orange-red calcium nodules was observed post-transfection of osteoblasts with miR-375 mimics. Images were acquired under a microscope at x400 magnification. (C) ALP activity and extracellular matrix mineralisation levels. (D) Cell proliferative activity. (E) Expression of osteoblast activity-associated marker genes. Scale bars, 25 μ m. * P <0.05 and ** P <0.01 vs. control. ALP, alkaline phosphatase; BSP, bone sialoprotein; miR-375, microRNA-375; OB, osteoblast; OD, optical density; OPG, osteoprotegerin; OPN, osteopontin; RUNX2, runt-related transcription factor 2.

(P <0.01; Fig. 4C). Alizarin red staining revealed apparent orange-red calcium nodules in osteoblasts (Fig. 4B). Alizarin red quantification revealed that the extent of extracellular matrix

mineralisation in the miR-375 mimics-transfected cells was significantly higher compared with in the control group (P <0.05; Fig. 4C). Furthermore, the proliferative activity of osteoblasts

was significantly increased in the group transfected with miR-375 mimics ($P < 0.05$; Fig. 4D). RT-qPCR results revealed that osteoblasts transfected with miR-375 mimics overexpressed osteoprotegerin (OPG), osteopontin (OPN), runt-related transcription factor 2 (RUNX2) and bone sialoprotein (BSP) (Fig. 4E), which are osteoblast activity-associated marker genes.

Discussion

Johnstone *et al* previously isolated and extracted exosomes from reticulocyte culture medium; these membranous vesicles are released into the extracellular matrix by the fusion of cellular multivesicle bodies and cytoplasmic membranes (6). Studies have since revealed that most cells, including tumour cells, generate and secrete exosomes (21,22). Their roles are to carry proteins, lipids and nucleic acids from their parent cells to target cells, and therefore participate in the intercellular communication that regulates the tumour metastatic microenvironment (23). In the present study, morphological observation and particle size analysis were used to confirm that the cell-extracted particles had the characteristics of exosomes.

Exosomes contain various proteins, and DNA, mRNA, miRNA and long non-coding RNA molecules (24). The majority of exosomes harbour a common protein or protein family that can be used as exosome markers. These proteins include the following: The membrane-associated proteins CD9, CD63, CD81 and CD82; the cytoplasmic proteins Hsp70 and Hsp90; some important components of the internal body separation complex, including Alix and tumour susceptibility 101; the membrane transport and fusion proteins Rab and GTP; and membrane proteins, including Annexins (25,26). In the present study, five protein markers (CD9, CD63, CD81, Hsp70 and Alix) were selected as exosomal markers, whereas GM130 was used as a negative marker, as the cis-Golgi marker GM130 is only present in cell lysates. These results confirmed that the vesicles isolated from the conditioned media were exosomes based on their marker protein expression as the isolated exosomes were positive for the exosomal marker and negative for the cis-Golgi marker GM130.

The results revealed that the particles isolated from the cell supernatants presented all these markers, confirming that these particles were exosomes.

Altered levels of miRNAs have previously been associated with the development of PCa (27,28). Furthermore, exosomal miR-375 is closely related to the development of PCa. In addition, Huang *et al* identified miR-375 as a promising prognostic biomarker in castration-resistant PCa (29). Foj *et al* reported that miR-375 levels are significantly upregulated in the urinary exosomes of patients with PCa, thus suggesting that miR-375 may be used as a valuable biomarker in the detection and prognosis of PCa (30). In the present study, next-generation sequencing differential expression analysis demonstrated that the top three upregulated miRNAs in LNCaP-isolated exosomes were miR-375, miR-200c-3p and miR-141-3p compared with in RWPE-1-isolated exosomes. Furthermore, the top three downregulated miRNAs in LNCaP-isolated exosomes were miR-100-5p, miR-584-5p and miR-125b-1-3p compared with in RWPE-1-isolated exosomes. The RT-qPCR results revealed that the expression levels of exosomal miR-375

were significantly increased in PCa cells ($P < 0.05$), and that LNCaP-isolated exosomes presented increased expression levels of miR-375. These findings were in line with the high expression levels of miR-375 identified in exosomes from LNCaP cells and confirmed the association between exosomal miR-375 and PCa.

Bone metastasis is the most common complication in advanced stages of PCa, and the main cause of mortality in patients with PCa (31). This disease is characterised by bone lesions, particularly in the trunk bones. This topic has received significant interest in recent years. Various studies (32,33) have supported the theory of 'seed soil' put forward by Stephen Paget, which suggests that invasive tumour cells can only proliferate in microenvironments suitable for their growth, and that they form metastatic lesions in specific tissues and organs (34). The impact of the microenvironment on tumour growth and metastasis has also been revealed in another study, suggesting that tumour cells and osteoblasts can remotely interact with each other and promote the proliferation of one another (35). Increasing evidence suggests that the development of PCa is closely associated with the interaction of tumour cells and osteoblasts (36).

Osteoblasts are an important type of cell involved in the synthesis of bone matrix and mineralisation, bone growth and development, and regulation of damage and repair. These cells have been reported to serve an important role in the bone metastatic microenvironment. The differentiation and maturation of osteoblasts involve various factors, including miRNAs (37). In the present study, a high level of RFP fluorescence was observed in osteoblasts cultured with CMV-RFP-CD63-infected LNCaP cells, miR-375 levels in osteoblasts were significantly increased, and osteoblast proliferation was significantly enhanced. ALP is an extracellular enzyme secreted by osteoblasts that is used as an important index for the early differentiation of osteoblasts (38). The results of the present study revealed that ALP levels were increased in the cell cytoplasm following miR-375 mimics transfection.

Calcium nodules are important markers in the late stages of osteoblast differentiation and indicate the level of extracellular matrix mineralisation. Alizarin red staining is a common method used to observe the formation of these nodules and therefore determine the degree of osteoblast differentiation, since calcium ions in calcium nodules can be chelated with Alizarin red to form a red complex (39). The present results of Alizarin red staining revealed the deposition of orange-red calcium nodules in osteoblasts post-transfection. Quantitative analysis revealed that the level of extracellular matrix mineralisation by osteoblasts was significantly higher post-transfection than that in the control group ($P < 0.05$). Furthermore, compared with the control cells, miR-375 mimic-transfected osteoblasts exhibited significantly increased expression levels of OPG, RUNX2, OPN and BSP, which are associated with osteoblast activity and differentiation. These findings suggested that stimulating osteoblast activity may contribute to the development of bone metastasis in patients with PCa.

In conclusion, the present study confirmed that miR-375 was highly expressed in exosomes from the LNCaP cell line, and that the LNCaP-derived exosomes may preferentially reach osteoblasts and increase their levels of miR-375. In

addition, exosomal miR-375 may significantly promote osteoblast activity. The molecular mechanisms underlying the association of exosomal miR-375 with the activation and differentiation of osteoblasts, and the mechanism underlying bone metastasis in patients with PCa require further investigation.

Acknowledgements

Not applicable.

Funding

No funding was received.

Availability of data and materials

The datasets used and/or analyzed during the present study are available from the corresponding author on reasonable request.

Authors' contributions

SLL and YY contributed to the conception of the study. BL and NA contributed to analysis and manuscript preparation. SLL and NA performed the data analyses and wrote the manuscript. SYW and JJW helped perform the analysis and provided constructive discussions.

Ethics approval and consent to participate

The present study was approved by the Ethics Committee of The First Affiliated Hospital of Xi'an Medical University. Informed consent was obtained from all participants.

Patient consent for publication

Not applicable.

Competing interests

The authors declare that they have no competing interests.

References

- Ferlay J, Shin HR, Bray F, Forman D, Mathers C and Parkin DM: Estimates of worldwide burden of cancer in 2008: GLOBOCAN 2008. *Int J Cancer* 127: 2893-2917, 2010.
- Siegel RL, Miller KD and Jemal A: Cancer statistics, 2017. *CA Cancer J Clin* 67: 7-30, 2017.
- Suzman DL, Boikos SA and Carducci MA: Bone-targeting agents in prostate cancer. *Cancer Metastasis Rev* 33: 619-628, 2014.
- Larson SR, Zhang X, Dumpit R, Coleman I, Lakely B, Roudier M, Higano CS, True LD, Lange PH, Montgomery B, *et al*: Characterization of osteoblastic and osteolytic proteins in prostate cancer bone metastases. *Prostate* 73: 932-940, 2013.
- Rajpar S and Fizazi K: Bone targeted therapies in metastatic castration-resistant prostate cancer. *Cancer J* 19: 66-70, 2013.
- Johnstone RM, Adam M, Hammond JR, Orr L and Turbide C: Vesicle formation during reticulocyte maturation. Association of plasma membrane activities with released vesicles (exosomes). *J Biol Chem* 262: 9412-9420, 1987.
- Denzer K, Kleijmeer MJ, Heijnen HF, Stoorvogel W and Geuze HJ: Exosome: From internal vesicle of the multivesicular body to intercellular signaling device. *J Cell Sci* 113: 3365-3374, 2000.
- Gusachenko ON, Zenkova MA and Vlassov VV: Nucleic acids in exosomes: Disease markers and intercellular communication molecules. *Biochemistry (Mosc)* 78: 1-7, 2013.
- Soung YH, Ford S, Zhang V and Chung J: Exosomes in cancer diagnostics. *Cancers (Basel)* 9: 8, 2017.
- Zhou Y, Xia L, Lin J, Wang H, Oyang L, Tan S, Tian Y, Su M, Wang H, Cao D and Liao Q: Exosomes in nasopharyngeal carcinoma. *J Cancer* 9: 767-777, 2018.
- Ruivo CF, Adem B, Silva M and Melo SA: The Biology of Cancer Exosomes: Insights and New Perspectives. *Cancer Res* 77: 6480-6488, 2017.
- Zhou M, Chen J, Zhou L, Chen W, Ding G and Cao L: Pancreatic cancer derived exosomes regulate the expression of TLR4 in dendritic cells via miR-203. *Cell Immunol* 292: 65-69, 2014.
- Stevanato L, Thanabalasundaram L, Vysokov N and Sinden JD: Investigation of Content, Stoichiometry and Transfer of miRNA from Human Neural Stem Cell Line Derived Exosomes. *PLoS One* 11: e0146353, 2016.
- Greening DW, Gopal SK, Xu R, Simpson RJ and Chen W: Exosomes and their roles in immune regulation and cancer. *Semin Cell Dev Biol* 40: 72-81, 2015.
- Hashimoto K, Ochi H, Sunamura S, Kosaka N, Mabuchi Y, Fukuda T, Yao K, Kanda H, Ae K, Okawa A, *et al*: Cancer-secreted hsa-miR-940 induces an osteoblastic phenotype in the bone metastatic microenvironment via targeting ARHGAP1 and FAM134A. *Proc Natl Acad Sci USA* 115: 2204-2209, 2018.
- Corcoran C, Rani S and O'Driscoll L: miR-34a is an intracellular and exosomal predictive biomarker for response to docetaxel with clinical relevance to prostate cancer progression. *Prostate* 74: 1320-1334, 2014.
- Ye Y, Li SL, Ma YY, Diao YJ, Yang L, Su MQ, Li Z, Ji Y, Wang J, Lei L, *et al*: Exosomal miR-141-3p regulates osteoblast activity to promote the osteoblastic metastasis of prostate cancer. *Oncotarget* 8: 94834-94849, 2017.
- Costa-Silva B, Aiello NM, Ocean AJ, Singh S, Zhang H, Thakur BK, Becker A, Hoshino A, Mark MT, Molina H, *et al*: Pancreatic cancer exosomes initiate pre-metastatic niche formation in the liver. *Nat Cell Bio* 17: 816-826, 2015.
- Livak KJ and Schmittgen TD: Analysis of relative gene expression data using real-time quantitative PCR and the 2(-Delta Delta C(T)) method. *Methods* 25: 402-8, 2001.
- Möller A, House CM, Wong CS, Scanlon DB, Liu MC, Ronai Z and Bowtell DD: Inhibition of Siah ubiquitin ligase function. *Oncogene* 28: 289-296, 2009.
- Lazar E, Benedek T, Korodi S, Rat N, Lo J and Benedek I: Stem cell-derived exosomes—an emerging tool for myocardial regeneration. *World J Stem Cells* 10: 106-115, 2018.
- Messenger SW, Woo SS, Sun Z and Martin TFI: A Ca²⁺-stimulated exosome release pathway in cancer cells is regulated by Munc13-4. *J Cell Biol* 217: 2877-2890, 2018.
- Ge R, Tan E, Sharghi-Namini S and Asada HH: Exosomes in cancer microenvironment and beyond: Have we overlooked these extracellular messengers? *Cancer Microenviron* 5: 323-332, 2012.
- Yu S, Cao H, Shen B and Feng J: Tumor-derived exosomes in cancer progression and treatment failure. *Oncotarget* 6: 37151-37168, 2015.
- Mathivanan S, Fahner CJ, Reid GE and Simpson RJ: ExoCarta 2012: Database of exosomal proteins, RNA and lipids. *Nucleic Acids Res* 40 (Database Issue): D1241-D1244, 2012.
- Théry C, Ostrowski M and Segura E: Membrane vesicles as conveyors of immune responses. *Nat Rev Immunol* 9: 581-593, 2009.
- Bertoli G, Cava C and Castiglioni I: MicroRNAs as biomarkers for diagnosis, prognosis and therapeutics in prostate cancer. *Int J Mol Sci* 17: 421, 2016.
- Filella X and Foj L: miRNAs as novel biomarkers in the management of prostate cancer. *Clin Chem Lab Med* 55: 715-736, 2017.
- Huang X, Yuan T, Liang M, Du M, Xia S, Dittmar R, Wang D, See W, Costello BA, Quevedo F, *et al*: Exosomal miR-1290 and miR-375 as prognostic markers in castration-resistant prostate cancer. *Eur Urol* 67: 33-41, 2015.
- Foj L, Ferrer F, Serra M, Arévalo A, Gavagnach M, Giménez N and Filella X: Exosomal and non-exosomal urinary miRNAs in prostate cancer detection and prognosis. *Prostate* 77: 573-583, 2017.
- Rucci N and Angelucci A: Prostate cancer and bone: The elective affinities. *Biomed Res Int* 2014: 167035, 2014.

32. Keller ET, Zhang J, Cooper CR, Smith PC, McCauley LK, Pienta KJ and Taichman RS: Prostate carcinoma skeletal metastases: Cross-talk between tumor and bone. *Cancer Metastasis Rev* 20: 333-349, 2001.
33. Mohla S: Under-investigated area in prostate cancer: Cross talk between the bone microenvironment and prostate cancer bone metastasis. *J Cell Biochem* 91: 684-685, 2004.
34. Paget S: The distribution of secondary growths in cancer of the breast. 1889. *Cancer Metastasis Rev* 8: 98-101, 1989.
35. Engblom C, Pfirschke C, Zilionis R, Da Silva Martins J, Bos SA, Courties G, Rickelt S, Severe N, Baryawno N, Faget J, *et al*: Osteoblasts remotely supply lung tumors with cancer-promoting SiglecFhigh neutrophils. *Science* 358: pii: eaal5081, 2017.
36. San Martin R, Pathak R, Jain A, Jung SY, Hilsenbeck SG, Piña-Barba MC, Sikora AG, Pienta KJ and Rowley DR: Tenascin-C and Integrin $\alpha 9$ mediate interactions of prostate cancer with the bone microenvironment. *Cancer Res* 77: 5977-5988, 2017.
37. Papaioannou G, Mirzamohammadi F and Kobayashi T: MicroRNAs involved in bone formation. *Cell Mol Life Sci* 71: 4747-4761, 2014.
38. Yun HM, Park KR, Quang TH, Oh H, Hong JT, Kim YC and Kim EC: 2,4,5-Trimethoxydalbergiquinol promotes osteoblastic differentiation and mineralisation via the BMP and Wnt/ β -catenin pathway. *Cell Death Dis* 6: e1819, 2015.
39. Lee HS, Jung EY, Bae SH, Kwon KH, Kim JM and Suh HJ: Stimulation of osteoblastic differentiation and mineralisation in MC3T3-E1 cells by yeast hydrolysate. *Phytother Res* 25: 716-723, 2011.



This work is licensed under a Creative Commons Attribution-NonCommercial-NoDerivatives 4.0 International (CC BY-NC-ND 4.0) License.

RETRACTED